



## SEISMIC RELIABILITY ASSESSMENT OF LIQUID STORAGE TANKS

Konstantinos BAKALIS<sup>1</sup>, Dimitrios VAMVATSIKOS<sup>2</sup> and Michalis FRAGIADAKIS<sup>3</sup>

### ABSTRACT

Large-capacity atmospheric tanks are widely used to store liquids, such as oil or liquefied natural gas. The seismic risk of such industrial facilities is considerably higher compared to ordinary structures, since even some minor damage induced by a ground motion may have uncontrollable consequences, not only on the tank but also on the environment. Recent earthquakes have shown that heavy damage on tanks may lead to temporary loss of essential service, usually followed by leakage and/or fire. Therefore, a Performance-Based Earthquake Engineering (PBEE) framework should be employed for the seismic performance assessment of such critical infrastructure. Current design codes and guidelines have not fully adopted the PBEE concept, while its application to industrial facilities is still at the academic level. This study provides an insight on the seismic risk assessment of liquid storage tanks using a simplified performance-based oriented modelling approach. Appropriate system and component-level damage states are defined by identifying the failure modes that may occur during a strong ground motion. Fragility curves are estimated by introducing both aleatory and epistemic sources of uncertainty, thus providing a comprehensive methodology for the seismic risk assessment of liquid storage tanks.

### INTRODUCTION

Recent earthquakes have highlighted the need for innovative engineering concepts in order to mitigate the devastating consequences following a strong ground motion. Although extensive research takes place to date, earthquakes remain a major threat to the community both from a social and a financial point of view. The PBEE concept forms the state-of-the-art approach for evaluating the seismic risk, and it should be extended also to critical infrastructure, such as the liquid storage tanks found in industrial complexes.

Various approaches serve under this framework, ranging from simplified determinist to comprehensive probabilistic. In the latter case, the structural model adopted constitutes a key parameter for the successful performance evaluation, due to the computational time required during the analysis. This remark is highlighted for the case of atmospheric liquid storage tanks, where the simulation of the fluid-structure-interaction may result in complex finite element models (FEM) that require a considerable amount of time even for a single dynamic analysis (Kilic and Ozdemir, 2007). Similar studies have developed numerical approximations for the contained liquid (Talaslidis et al., 2004; Vathi et al. 2013), in an attempt to minimise the estimated computational time. Although the aforementioned FEM-based procedures may be able to capture complex modes of failure such as buckling, their suitability within a probabilistic framework may become computationally prohibitive. Still, at least two

---

<sup>1</sup> PhD Student, National Technical University of Athens, Greece, kbakalis@mail.ntua.gr

<sup>2</sup> Lecturer, National Technical University of Athens, Greece, divamva@mail.ntua.gr

<sup>3</sup> Lecturer, National Technical University of Athens, Greece, mfrag@mail.ntua.gr

studies have attempted to develop simplified simulation techniques that blend efficiency and accuracy. Malhotra and Veletsos (1994a,b,c) presented a simplified model for the two-dimensional (2D) analysis of liquid storage tanks, while, Cortes et al. (2012) developed a model based on rigid beams and equivalent springs that can be used for rapid dynamic analysis. Still, neither of the two can be easily applied out-of-the-box with commercial software: The first approach is based on custom-made analysis software while the second needs FEM results for calibration (originally taken from the NZEE (2009) standards by the authors).

Our aim is to improve upon the existing body of work by offering a surrogate model that can be implemented with minimum effort with both anchored and unanchored tanks, for application within a PBEE framework using either static or dynamic analysis methods. At the same time, a robust fragility evaluation approach is presented to estimate the seismic risk involved in liquid storage tanks.

**MODELLING**

It has been widely accepted within the Earthquake Engineering community that the simulation procedure of a structural system should provide structural models that not only offer valid analysis results, but also minimise the estimated computational time. Even though a few runs may be enough to optimise the design of a structure, determining a performance level for an existing structural system requires a fair amount of scenarios to be considered, which may in turn affect not only delivery times but also the quality of the study. In that sense, the response of liquid storage tanks can be idealised using a two-degree-of-freedom (2DOF) system, where the two masses (impulsive and convective) are considered to be decoupled (Malhotra et al., 2000; Priestley et al., 1986). The geometric and modal characteristics of the hydrodynamic problem are determined using equivalent parameters for the impulsive and convective masses. For the purpose of this study, the recommendations of EC8 (CEN, 2004) are adopted featuring Part 4 (CEN, 2006), where the design of tanks is discussed in detail. Under the assumption that the impulsive pressure is acting on the tank walls only, one may obtain estimates for parameters such as the natural period coefficients ( $C_i$  and  $C_c$ ), the masses ( $m_i$  and  $m_c$ ) and the effective height components ( $h_i$  and  $h_c$ ). These parameters are distinguished with the aid of subscripts “*i*” and “*c*” denoting “impulsive” and “convective”, respectively. Other studies, however, have shown that the contribution of the convective mass to the overall response of the structure can be ignored, as the impulsive mass is held responsible for the majority of the damage that tanks suffer during a strong ground motion event (Malhotra, 1997; Vathi et al., 2013). Decoupling shall form the basis of the procedure adopted, thus providing the ability for a robust simulation tool that is easy to implement compared to the time-consuming three-dimensional finite element models.

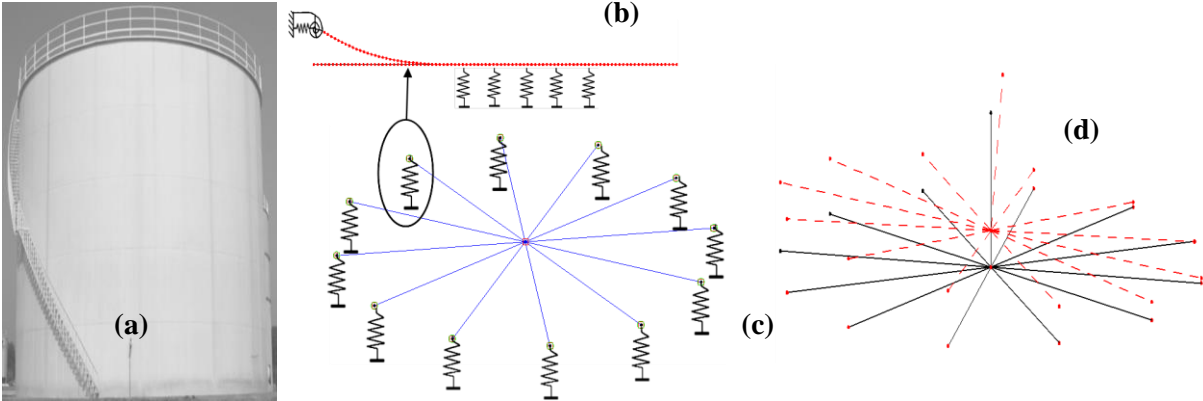


Figure 1. (a) Atmospheric tank, (b) Strip model, (c) Base plate model, (d) Simplified model of the entire tank

The modelling approach presented herein is based on previous work of Malhotra and Veletsos, where the analysis procedure can be divided into two distinct steps. The first step comprises the analysis of a single base plate strip in order to determine its uplifting resistance (Malhotra and Veletsos, 1994a), while the second evaluates the entire base plate response in terms of moment-rotation and moment-uplift curves. The second step uses the products of the first as an input through vertical edge springs (Malhotra and Veletsos, 1994b). According to Malhotra and Veletsos (1994c), the results provided by the first step may also be used for the evaluation of both the static and the dynamic response of the full tank model. A very interesting feature of the model is the ability to simulate not only the unanchored but also the partially anchored problem of liquid storage tanks, where every equivalent “edge spring” is assumed to carry a number of bolts, equally distributed along the circumference. Fig.1 summarises the modelling procedure suggested. The base plate of the tank shown in Fig.1(a) (Amiri and Sabbagh-Yazdi, 2011) is modelled as a single strip in Fig.1(b) before the entire base plate (Fig.1(c)) or the full tank model (Fig.1(d)) is analysed.

### Case study example

In order to validate our modelling approach, we shall compare it against a more accurate 3D finite element model. The tank analysed by Vathi et al. (2013), assumed to be 95% filled with water, was thus adopted as a testbed. Its properties are summarised in Table.1.

Table 1. Properties of the tank examined by Vathi et al. (2013)

	Variable description	Notation (units)	Numerical values
<b>Tank properties</b>	Radius	$R_t$ (m)	13.9
	Height	$h_t$ (m)	16.5
	Wall thickness per course	$t_w$ (mm)	6.4/10.0/14.0/17.7
	Base plate thickness	$t_b$ (mm)	6.4
	Annular ring thickness	$t_a$ (mm)	8.0
	Roof mass	$m_r$ (ton)	40
	Yield strength	$f_y$ (MPa)	235
	Steel Young's Modulus	$E_s$ (GPa)	210
<b>Fluid properties</b>	Height	$h_f$ (m)	15.7
	Density	$\rho_f$ (kg/m <sup>3</sup> )	1,000

### Modelling of unanchored tanks

For the first step of the modelling procedure, a single strip of the tank's base plate will be tackled. As shown in Fig.1(b), the base plate is discretised into 300 force-based fibre beam-column elements (element length in the order of  $15t_b$ ). A uniaxial elastoplastic material is assigned to the fibres, in order to capture the inelastic behaviour of the base plate during uplift. Geometric nonlinearities are also taken into account through a co-rotational formulation. Neglecting large-displacement nonlinearities in the response may result in what Malhotra and Veletsos (1994a) call the “bending solution”, which deviates from the true solution as catenary string effects are ignored. This means that as the edge of the tank is uplifted, the base is not only bent but also tensioned and thus straightened. In other words, the plastic rotation has an actual maximum limit that it will not exceed. A direct mapping between the uplift ( $w$ ), the separation length ( $L$ ) and the plastic rotation ( $\theta_{pl}$ ) is suggested by EC8 (CEN, 2006) in accordance with the strip analysis uplifting response:

$$g_{pl} = \frac{2w}{L} - \frac{w}{2R} \quad (1)$$

To model the foundation of the tank, Winkler springs are used. The unanchored tank is assumed to rest on a concrete slab, thus implying a base/soil flexibility of  $E_w=1.0$  GPa. The Winkler springs are also assigned an elastic-no-tension material which is suitable for the simulation of the uplifting of the

tank's base plate. As the tank is uplifted, local buckling tends to develop at the base-plate-tank-wall junction. In order to capture the plate-wall interaction, edge rotational springs are also provided and their stiffness for a given width of the strip ( $b$ ) is determined following the suggestions found in Malhotra and Veletsos (1994a), as shown in Fig.2.

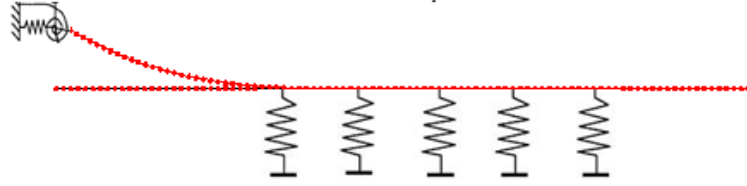


Figure 2: Base plate strip model

$$k_{\theta\theta} = \frac{Ebt_w^2(t_w / R_t)^{1/2}}{2[3(1 - \nu^2)]^{3/4}} \quad (2)$$

$$k_{\theta u} = \frac{Ebt_w(t_w / R_t)^{1/2}}{2[3(1 - \nu^2)]^{1/2}} \quad (3)$$

$$k_{uu} = \frac{Eb(t_w / R_t)^{3/2}}{2[3(1 - \nu^2)]^{1/4}} \quad (4)$$

$k_{\theta\theta}$  is the rotational and  $k_{uu}$  the translational (axial) edge stiffness. The term  $k_{\theta u}$  represents the interaction of rotation and translation and it will be neglected herein as it cannot be incorporated using uniaxial springs. Either way, sensitivity analyses have shown that its effect is not significant.

A concentrated moment and axial load are applied on the plate boundary in order to simulate the effect of the pressure acting on the tank wall. These actions induce some local uplifting on a narrow area next to the edge of the base plate. An overview of the base plate strip model is given below, while the uplifting resistance and plastic rotation are presented in Fig.3. According to Fig.3(a), the strip model yields by the time some minor uplifting is induced. As the model is further uplifted, some stiffness degradation takes place, while once the 0.2m limit is exceeded, the response becomes significantly stiffer due to “string” effects. Fig.3(b) presents a comparison between the recorded model plastic rotation and the corresponding response estimated according to EC8. The latter is presented using the direct results of Eq.(1) (dashed curve), where once the ultimate plastic rotation is reached the response suddenly begins to decrease. The appearance of smaller plastic rotations for larger uplifts simply indicates a lack of monotonicity, rather than a reduction per se of the response: At each uplift value, one should consider the peak value of plastic rotation that has been encountered through the entire loading history up to that point, essentially placing a case-specific cap on the maximum achievable plastic rotation, but no net reduction with uplift. This is shown by the bilinear solid curve in Fig.3b. It is evident that there is a considerable variation between the actual model-predicted values and the EC8 approach, and even though one may argue that the EC8 equation is built upon a series of assumptions, such as the length of the plastic hinge developed, properly solving the actual problem requires a detailed modelling approach which is beyond the scope of this study. Thus, having no further data to compare against, the EC8 approach is adopted for the plastic rotation response of the model.

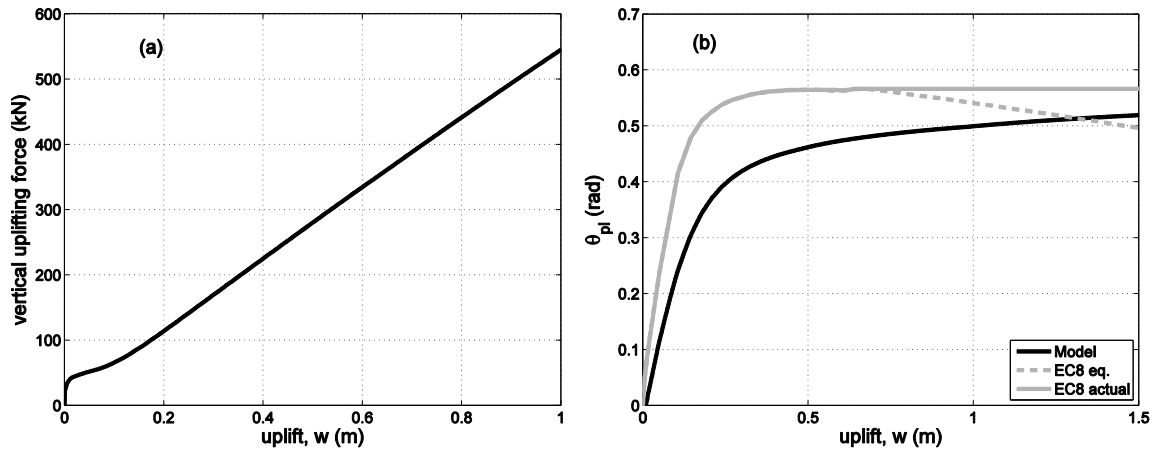


Figure 3. (a) Base plate strip uplifting resistance and (b) edge uplift versus plastic rotation. Of the two EC8 curves, the dashed line is the prediction of the instantaneous value via Eq.(1) while the solid line represents the consideration of the maximum encountered plastic rotation.

In the second step of the modelling procedure, the uplifting rigidity of the entire base plate is evaluated by applying an incremental moment load on it. Following the ideas of Malhotra & Veletsos (1994), the base plate is simulated using an even number of beam-spokes (Fig.1c), whose properties carry a large Young's modulus, such that the rigid motion of the system is ensured. According to Malhotra and Veletsos (1994b), elastic beam-column elements used for the beam-spokes are assigned a uniform width ( $b_w$ ), where 'n' is the number of beams used for the modelling of the base plate:

$$b_w = \frac{2\pi R}{n} \quad (5)$$

The nonlinear behaviour of the system is induced through zero-length springs that connect the base plate to the ground, with their properties already defined during the base plate strip analysis. An elastic nonlinear material, e.g., ElasticMultilinear in OpenSees (Mazzoni et al., 2005), is used to idealise the uplift resistance of the strips. The stress-strain relationship given by the multi-linear curve implies a complex nonlinear-elastic behaviour for the soil-tank-interaction, according to the findings of Malhotra and Veletsos (1994c). The base plate model and its deflected shape are presented in Fig.1(c).

Fig.4 presents a comparison of the overturning moment obtained with our model and with the detailed finite element model of Vathi et al. (2013). Good agreement between the two curves is observed, although some discrepancies are found in the post yield zone, and also when a base rotation of  $\theta=0.02$  rad is exceeded. The modelling procedure developed in this study presents a reasonable match close to the yield point. Moreover, it seems to underestimate the response of the unanchored tank in the post-yield zone, while once the base rotation exceeds the 0.01 rad the slope of the capacity curve increases with respect to the fitted curve. This implies a slightly stiffer approach. In all, the modelling procedure adopted provides a good match to the FEM solution, since the differences found are less than 15%.

The entire tank is modelled using the outcome of the two aforementioned steps. Following the procedure outlined in the base plate analysis section, a mass representing the impulsive component of the liquid is connected to the base using an elastic beam-column element, whose properties are estimated using the equivalent stiffness that corresponds to the fundamental (impulsive) period and mass. The deflected shape of the full tank model is presented in Fig.1(d).

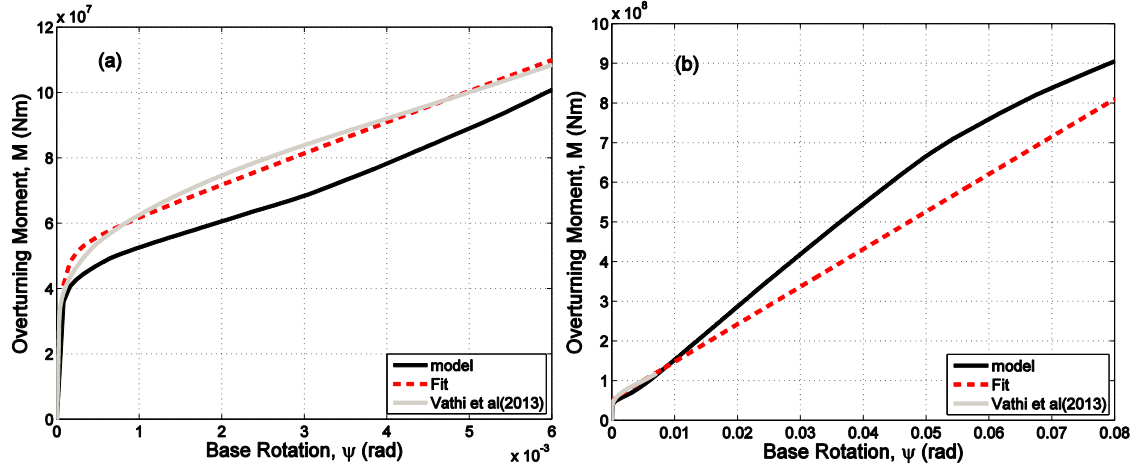


Figure 4. Base plate rotational resistance: (a) close to the yield point, (b) for larger deformations.

## Modelling of anchored tanks

Appropriate modifications are necessary for modelling anchored and partially anchored liquid storage tanks. The tank is anchored to the ground using vertically-oriented uniaxial springs, one at the end of each beam spoke. Each spring is assumed to carry ' $N$ ' number of bolts, equally distributed along the beam-spoke's width ( $b_w$ ). As a result, the stiffness assuming rigidity for the flange connection may be calculated using Eq.(6), where  $E_s$  is the steel Young's modulus,  $A_b$  is the total area of the bolts required and  $L_b$  their respective length. The anchoring springs are thus located on the circumference of the base plate and are introduced to the model through elastoplastic no-compression material behavior, where the tension yield point is assumed to resist a proportion (25% for our case study) of the fluid overturning moment. A more faithful representation of anchor behaviour may be achieved (a) by adding a limiting ultimate displacement  $\delta_u$  to indicate fracture and (b) by using damageable "gap" materials for the springs, e.g., the Elastic-Perfectly Plastic Gap Material of Opensees (Mazzoni et al., 2005). The aforementioned material offers the ability to accumulate damage on yielding anchors in the form of permanent elongation that causes a characteristic displacement gap before tension can be developed in reloading. The axial stiffness of each individual anchor (assuming a perfectly rigid connecting flange) can be estimated as:

$$K_b = \frac{E_s A_b}{L_b} \quad (6)$$

In order to obtain a deeper understanding on the response of partially anchored systems, a parametric study is conducted using a range of ultimate displacements for the anchored connections. Following the concept outlined above, the pushover as well as the time history analysis are employed for ultimate displacement values ranging from  $\delta_u = 1\text{cm}$  to  $\delta_u = 20\text{cm}$ . The results presented in Fig.5(a) show the edge uplift versus the horizontal force that is incrementally applied on the impulsive mass of the tank model. Fig.5(b) presents the corresponding time history responses for a scaled version of the El-Centro record. It is evident that as the ultimate displacement of the anchorage increases, the system capacity increases as well. At the same time, the response of the partially anchored system seems to change significantly once the anchors begin to fail. For low ultimate displacement values, the majority of anchors fail almost simultaneously, whereas as  $\delta_u$  approaches 20cm, a progressive fracture of the connections (followed by a sudden drop of the system's stiffness) takes place until the response becomes similar to that of the unanchored tank.

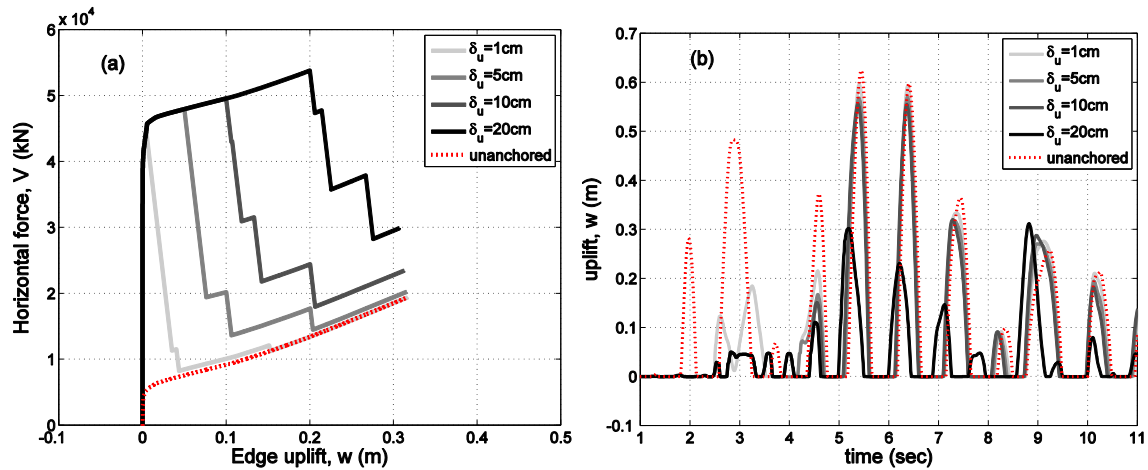


Figure 5. Parametric study for partially anchored tanks: (a) Pushover analysis, edge uplift versus horizontal force, (b) Time history analysis, time versus edge uplift.

## LOSS-ORIENTED DAMAGE CLASSIFICATION

Field investigations after major earthquake have revealed a variety of failure modes on atmospheric tanks. The most common types of failure are shell buckling, base sliding and sloshing damage to the upper tank shell and roof. EC8-part 4 (CEN, 2006) provide special provisions for these modes of failure (Vathi et al., 2013). During strong ground motion events, hydrostatic and hydrodynamic effects may lead to high internal pressure on the tank walls. Overturning for those thin shell structures is resisted by axial compressive stresses in the wall. Even though high pressure may increase the capacity against buckling, local yielding may trigger an elastic-plastic buckling failure around the lower course of the tank's perimeter, known as the "Elephant's Foot Buckling" (EFB). When partial uplifting is allowed, either for design purposes or due to poor detailing of the anchors, the rotation of the plastic hinge in the tank base should not exceed a certain rotational capacity, specified in EC8. Moreover, the excitation of the long period convective mass may cause sloshing of the contained liquid, which may in turn damage the upper parts of the tank (roof, upper course). Therefore, the approach for assessing the capacity of these structure substantially differs from that of buildings (i.e. steel moment frames).

The most damaging failure modes are these that may result in loss of containment, while other modes are mainly confined to structural damage without leakage. Thus, for the performance-based assessment of atmospheric tanks we consider three damage states of increasing severity, namely minor (DS1), severe without leakage (DS2) and loss of containment (DS3). Although this classification may seem reasonable for roughly understanding the extent of damage, the accurate assessment of loss may become tricky as, for example, the different mechanisms involved in a single damage state may be associated with varying degrees of loss. For instance, the sloshing height response represents relatively easy-to-repair damage at the top of the tank, compared to an exceedance of a plastic rotation limit at the base. Thus, it becomes more informative to also classify damage based on the actual component that has failed. Fig.6 presents the associated failure modes on the median Incremental Dynamic Analysis (IDA) curve (Vamvatsikos and Fragiadakis, 2009) for both an unanchored and a partially anchored system. It is evident that a component-based classification of damage is quite informative, where the upper course of the tank (SL=sloshing), its lower course (EFB), the base plate ( $\theta_{pl}$ =plastic rotation), and the anchors (AN=yielding/fracture of anchors) are individually examined. Table.2 presents the median damage state capacities along with their associated dispersions and engineering demand parameters (EDP). Due to lack of relevant data, the FEMA (2012) guidelines are adopted: The proposed strength (EFB), ductility (plastic rotation and anchorage yield/fracture) and displacement-based (sloshing) procedures are employed for the damage state dispersion estimation.

The classification outlined above may indeed offer a comprehensive reliability assessment procedure for a single liquid storage unit. Under a strong earthquake excitation, however, a group of similar structural systems is expected to suffer consequences ranging from limited structural damage to loss of containment, and thus a global damage state classification should also be considered. In that

sense, DS1 shall represent some minor damage induced by a sloshing wave height of the contained liquid equal to the freeboard. DS2 shall refer to severe damage at any component of the tank without leakage, where the exceedance of either a sloshing wave height equal to 1.4 times the available freeboard or a plastic rotation of 0.2 rad at the base plate shall trigger the damage state violation. DS3, finally, shall provide information on the loss of containment through the exceedance of either the axial EFB capacity ( $N_{\text{EFB}}$ ) or the base plate plastic rotation of 0.4 rad. As far as partially anchored systems are concerned, the yielding of the anchors may also be considered for DS1, while the fracture of the connection for DS2, as shown in Table.3.

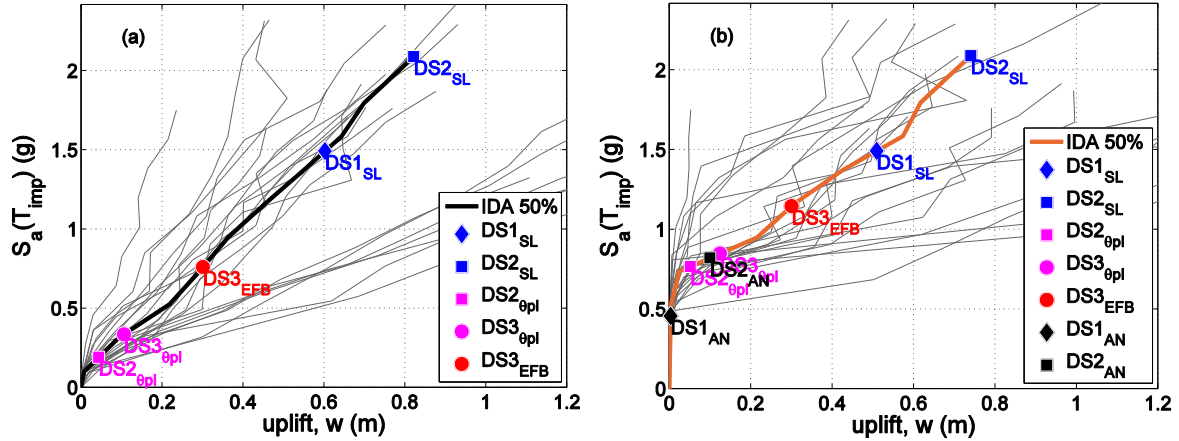


Figure 6: Single record and median Incremental Dynamic Analysis curves for an (a) Unanchored & (b) Partially Anchored Tank ( $\delta_u=10\text{cm}$ )

Table 2: Component-based Damage State classification

Component	Damage State Classification			
	Notation	Median Capacity		Dispersion
		$\hat{E}DP_c$	Reference	
Upper tank course	DS1 <sub>SL</sub>	$1.0 \times h_{\text{freeboard}}$ (m)	API-650 (2007)	0.20
	DS2 <sub>SL</sub>	$1.4 \times h_{\text{freeboard}}$ (m)	API-650 (2007)	0.20
Lower tank course	DS3 <sub>EFB</sub>	$N_{\text{EFB}}$ (kN)	CEN (2006)	0.31
Anchors	DS1 <sub>AN</sub>	Anchorage yielding $\delta_y$ (m)	Engineering Judgment	0.51
	DS2 <sub>AN</sub>	Anchorage fracture $\delta_u$ (m)	Engineering Judgment	0.51
Base plate	DS2 <sub>theta pl</sub>	0.2 (rad)	CEN (2006)	0.51
	DS3 <sub>theta pl</sub>	0.4 (rad)	Cortes et al. (2012)	0.51

Table 3: Global Damage States and their associated capacities for unanchored and partially anchored tanks (CEN, 2006; Cortes et al., 2012)

Tank Description	Damage State ( $DS_i$ )	Limit State Capacities
Unanchored	DS1	$1.0 \times h_{\text{freeboard}}$
	DS2	$1.4 \times h_{\text{freeboard}}$ or $\theta_{pl}=0.2$ rad
	DS3	$N_{\text{EFB}}$ or $\theta_{pl}=0.4$ rad
Partially Anchored	DS1	$1.0 \times h_{\text{freeboard}}$ or Anchorage yielding ( $\delta_y$ )
	DS2	$1.4 \times h_{\text{freeboard}}$ or $\theta_{pl}=0.2$ rad or Anchorage fracture ( $\delta_u$ )
	DS3	$N_{\text{EFB}}$ or $\theta_{pl}=0.4$ rad

## SEISMIC FRAGILITY ASSESSMENT

In order to calculate the seismic risk of liquid storage tanks the variables that govern the response of the tank are identified and are considered probabilistically. The parameters considered are the geometric characteristics of the tank and the type of connection to the ground. The limit-state capacities of these parameters are defined according to the literature. A total of three tanks with fluid-height-over-radius

ratios ranging from 1.13 to 3.30 is considered (Fig.7, Table.4), and Incremental Dynamic Analysis (IDA, Vamvatsikos and Cornell (2002)) is employed in order to obtain each tank's response for different levels of intensity. A set of 22 pairs of records (far-field ground motion set, FEMA (2009)) is used and a suitable scale factor is adopted such that the system's impulsive period spectral acceleration is assigned values ranging from 0.1g to 2.0g. During the dynamic analysis procedure, key parameters such as the base uplifting, the sloshing height, the base plate plastic rotation and the axial force triggering the Elephant's Foot Buckling are recorded in order to form a set of data that will help us estimate the seismic risk involved in liquid storage tanks.

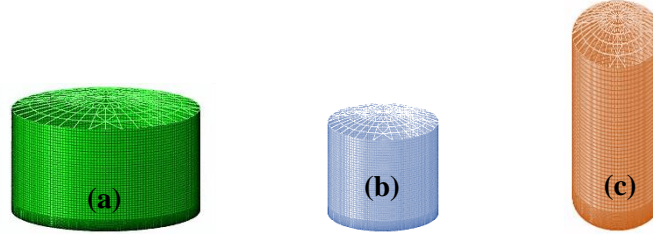


Figure 7: Case studies examined, (a) Tank A, (b) Tank B and (c) Tank C

Table 4: Geometric characteristics for the case studies examined

Tank	Reference	R (m)	$h_i$ (m)	$t_w$ per course (mm)	$t_b$ (mm)	Fluid height $h_f$ (m)	Freeboard (m)	$h_f/R$
A	Vathi et al. (2013)	13.9	16.5	6.4/10.0/14.0/17.7	6.4	15.675	0.825	1.13
B	Malhotra and Veletsos (1994c)	6.10	11.3	4.8/6.4/8.0/9.6	4.8	10.537	0.565	1.76
C	Koller and Malhotra (2004)	5.75	20.0	6.9	7.0	19.0	1.0	3.30

A suitable intensity measure (IM) is employed in order to correlate the varying ground motion intensity with the engineering demand parameters, which provide information on the damage a structure has suffered. An EDP-based fragility estimation methodology is adopted, where the probability of exceeding a certain limit state capacity for a given level of intensity may be calculated through the ratio of the sum of events that overcome the aforementioned capacity over the number of records used for the IDA. The EDP-based methodology forms a very simple procedure within a probabilistic framework, where the sample capacities are considered lognormally distributed around each limit state median capacity. The probability that the demand exceeds the median limit state capacity, given the intensity measure, may be calculated through the standard normal cumulative distribution function  $\Phi$  as shown in Eq.(7), where  $\hat{EDP}_c$  is the median limit state capacity,  $\hat{EDP}_d$  is the median demand given IM and  $\beta_{EDP_c}^2$ ,  $\beta_{EDP_d}^2$  their associated dispersions.

$$P(\hat{EDP}_c < \hat{EDP}_d | IM) = \Phi \left( \frac{\ln \hat{EDP}_d(IM) - \ln \hat{EDP}_c}{\sqrt{\beta_{EDP_c}^2 + \beta_{EDP_d}^2}} \right) \quad (7)$$

In order to accurately assess the seismic risk involved in liquid storage tanks, an intensity measure that characterises the structural system's response in an optimal manner must be identified. There has been a lot of discussion within the Earthquake Engineering community regarding which intensity measure better represents the structural response during the seismic risk assessment procedure. According to Luco and Cornell (2007) and Shafieezadeh et al. (2012), the answer to this question is not distinct, as certain parameters involved in a structural system may significantly affect its response, especially when the first-mode load-pattern is not applicable. For the case of liquid storage tanks, the peak ground acceleration (PGA) is a reasonable choice due to the impulsive load pattern adopted in the modelling procedure, even though its convective response can only be accurately estimated through the corresponding convective spectral acceleration. As with the majority of complex structural systems, it is unlikely that a single IM can adequately capture the response and hence other alternatives must be

considered. This is an interesting problem that requires a thorough discussion and despite it is beyond the scope of this study, it is expected to be covered in future direction of our research.

Table.5 summarises the entire seismic fragility assessment procedure. Fragility parameters such as the median intensity measure ( $IM_{50\%}$ ) response and the associated dispersion ( $\beta$ ) are provided for the corresponding fragility curve construction. The dominant failure mode (DFM) as well as the order each damage state appears during a strong ground motion, are also provided in order to highlight the complexity involved in cylindrical liquid storage systems. Special attention is paid to the compound system-level damage states, where a simple Monte Carlo integration is required to estimate the associated probability of exceedance. An example of the final fragility product for DS2 and DS3 is presented in Fig.8 for the unanchored tank A. It appears that although the plastic rotation clearly dominates the response for DS2, a similar conclusion cannot be drawn for DS3 as the dominant failure mode depends on the IM level, and hence is deemed *inconclusive*.

The performance evaluation developed herein presents the response of three tanks, with their geometric characteristics ranging from broad to slender structural systems. It appears that despite the sloshing mode representing the entire damage for all unanchored systems regarding DS1, the corresponding response for partially anchored tanks is dominated by the yielding of anchors, for considerably smaller median PGA estimates. DS2 on the other hand, reveals the plastic rotation as the dominant failure mode for every case of unanchored tanks, while for the case of partially anchored systems the prevalent response is deemed inconclusive. The dominant mode of failure that controls DS3 for Tank A is also inconclusive, while the remaining cases develop the loss of containment damage state once the EFB capacity is exceeded. The beneficial effect of anchors is also highlighted through the seismic fragility estimation for DS2 and DS3, where each failure mode is developed for significantly higher intensities. Finally, another major conclusion that can be drawn from the assessment procedure, is the fact that the damage states developed do not follow a priori the traditional order which dictates that increasing intensities result in increasing levels of damage. The issue of non-sequential damage states does not alter the well-known probability of exceedance estimation methodology, yet it highlights the uncertainties involved in the reliability assessment of complex structural systems.

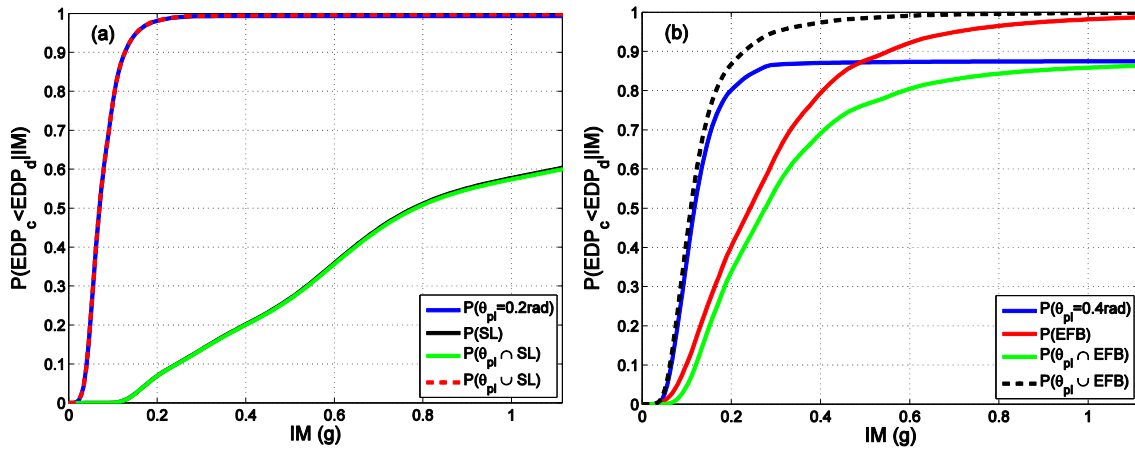


Figure 8: Compound damage states for the unanchored tank A: (a) DS2 & (b) DS3

Table 5: Seismic fragility assessment for the tanks examined

Tank	DS1			DS2			DS3			Order of DSi
	$IM_{50\%}$ (g)	$\beta$	DFM	$IM_{50\%}$ (g)	$\beta$	DFM	$IM_{50\%}$ (g)	$\beta$	DFM	
Unanchored A	0.507	0.878	SL	0.069	0.447	$\theta_{pl}$	0.109	0.477	inconclusive	2-3-1
Anchored A	0.139	0.386	AN	0.246	0.250	inconclusive	0.303	0.298	inconclusive	1-2-3
Unanchored B	0.507	0.780	SL	0.117	0.554	$\theta_{pl}$	0.121	0.417	EFB	3-2-1
Anchored B	0.322	0.532	inconclusive	0.577	0.515	inconclusive	0.724	0.349	EFB	1-2-3
Unanchored C	0.512	0.627	SL	0.098	0.788	$\theta_{pl}$	0.042	0.921	EFB	3-2-1
Anchored C	0.164	0.436	AN	0.369	0.323	inconclusive	0.285	0.665	EFB	1-3-2

## CONCLUSIONS

A reliability assessment methodology has been developed for liquid storage tanks based on a surrogate, yet robust, beam-element model. Following the identification of failure modes through Incremental Dynamic Analysis, a local as well as a global damage state classification is performed, favouring the seismic risk assessment of either a single liquid storage system or an entire group of tanks, respectively. The parametric study conducted utilises global damage states under a simplified probabilistic framework in order to assess the risk involved in liquid storage tanks. Fragility parameters are provided along with the dominant failure mode for each damage state. Non-sequential damage states are finally revealed, and the associated effect on the assessment methodology is discussed.

## ACKNOWLEDGEMENTS

This research has been co-financed by the European Union (European Social Fund – ESF) and Greek national funds through the Operational Program "Education and Lifelong Learning" of the National Strategic Reference Framework (NSRF) - Research Funding Program: **THALES**. Investing in knowledge society through the European Social Fund.

## REFERENCES

- Amiri M, and Sabbagh-Yazdi S R (2011) "Ambient vibration test and finite element modeling of tall liquid storage tanks", *Thin-Walled Structures*, 49(8):974–983
- API-650 (2007) *Seismic Design of Storage Tanks - Appendix E, Welded Steel Tanks for Oil Storage*. American Petroleum Institute, 11th Edition, Washington, D.C.
- CEN (2004) *Eurocode 8 : Design of structures for earthquake resistance - Part 1: General rules, seismic actions and rules for buildings (EN 1998-1:2004)European Standard NF EN* (Vol. 1). CEN, Brussels
- CEN (2006) *Eurocode 8: Design of structures for earthquake resistance–Part 4: Silos, tanks and pipelines European Committee for Standard* (Vol. 3). Brussels
- Cortes G, Prinz G S, Nussbaumer A, and Koller M G (2012) "Cyclic Demand at the Shell-Bottom Connection of Unanchored Steel Tanks", *Proceedings of the 15th World Conference on Earthquake Engineering*. Lisboa, Portugal
- FEMA (2009) *Quantification of Building Seismic Performance Factors*. FEMA P-695, prepared by Applied Technology Council for Federal Emergency Management Agency, Washington, D.C.
- FEMA (2012) *Seismic Performance Assessment of Buildings* (Vol. 1). FEMA P-58, prepared by the Applied Technology Council for the Federal Emergency Management Agency, Washington D.C
- Kilic S, and Ozdemir Z (2007) "Simulation of Sloshing Effects in Cylindrical Containers under Seismic Loading", *Proceedings of the 6. LS-DYNA Anwenderforum* (pp. I–I–9 – I–I–20)
- Koller M G, and Malhotra P K (2004) "Seismic Evaluation of Unanchored Cylindrical Tanks", *Proceedings of the 13th World Conference on Earthquake Engineering*. Vancouver, Canada
- Luco N, and Cornell C A (2007) "Structure-Specific Scalar Intensity Measures for Near-Source and Ordinary Earthquake Ground Motions", *Earthquake Spectra*, 23(2):357–392
- Malhotra P K (1997) "Seismic Response of Soil-Supported Unanchored Liquid-Storage Tanks", *Journal of Structural Engineering*, 123(4):440–450
- Malhotra P K, and Veletsos A S (1994a) "Beam Model for Base- Uplifting Analysis of Cylindrical Tanks", *Journal of Structural Engineering*, 120(12):3471–3488
- Malhotra P K, and Veletsos A S (1994b) "Uplifting Analysis of Base Plates in Cylindrical Tanks", *Journal of Structural Engineering*, 120(12):3489–3505
- Malhotra P K, and Veletsos A S (1994c) "Uplifting Response of Unanchored Liquid- Storage Tanks", *Journal of Structural Engineering*, 120(12):3525–3547
- Malhotra P K, Wenk T, and Wieland M (2000) "Simple Procedure for Seismic Analysis of Liquid-Storage Tanks", *Structural Engineering International*, 10(3):197–201
- Mazzoni S, McKenna F, Scott M H, and Fenves G L (2005) "OpenSees command language manual", *Pacific Earthquake Engineering Research Center*. PEER, CA
- NZEE (2009) *Seismic Design of Storage Tanks*. New Zealand National Society for Earthquake Engineering Wellington, New Zealand

- Priestley M J N, Wood J H, and Davidson B J (1986) "Seismic Design of Storage Tanks", *Bulletin of the New Zealand Society for Earthquake Engineering*, 19(4):272–284
- Shafieezadeh A, Ramanathan K, Padgett J E, and DesRoches R (2012) "Fractional order intensity measures for probabilistic seismic demand modeling applied to highway bridges", *Earthquake Engineering & Structural Dynamics*, 41(3):391–409
- Talasilidis D G, Manolis G D, Paraskevopoulos E, Panagiotopoulos C, Pelekasis N, and Tsamopoulos J a. (2004) "Risk analysis of industrial structures under extreme transient loads", *Soil Dynamics and Earthquake Engineering*, 24(6):435–448
- Vamvatsikos D, and Cornell C A (2002) "Incremental dynamic analysis", *Earthquake Engineering & Structural Dynamics*, 31(3):491–514
- Vamvatsikos D, and Fragiadakis M (2009) "Incremental dynamic analysis for estimating seismic performance sensitivity and uncertainty", *Earthquake Engineering & Structural Dynamics*, 39(2):141–163
- Vathi M, Pappa P, and Karamanos S A (2013) "Seismic Response of Unanchored Liquid Storage Tanks", *Proceedings of the Pressure Vessels & Piping Division Conference* (pp. 1–10). Paris, France